0026-895X/94/010074-10$03.00/0

MOLECULAR PHARMACOLOGY, 45:74-83

Conformers of Acetylcholinesterase: A Mechanism of Allosteric Control

JEFFREY L. TAYLOR, RICHARD T. MAYER, and CHESTER M. HIMEL[1]

Department of Entomology, University of Georgia, Athens, Georgia 30602 (J.L.T., C.M.H.), Department of Pharmacology and Experimental Therapeutics, School of Medicine, University of Maryland, Baltimore, Maryland 21201 (C.M.H.), USDA, ARS, SAA, Horticultural Research Laboratory, Orlando, Florida 32803 (R.T.M.)

Received September 30, 1992; Accepted October 20, 1993

SUMMARY

Rate control in acetylcholinesterase (AChE) involves a single anionic site whose anionic center controls rate-related biochemical and conformational changes in the E (free enzyme) and EA (acylated enzyme) conformers. Change in conformer structure and biochemistry affect binding, acylation, and hydrolysis. It is significant that the anionic-esteratic intersite distance is not altered during conformer change as E is converted to EA. In this enzyme system, cationic acetylcholine and anionic AChE are true structural, functional, and biochemical counterparts. The anionic center in the E conformer lies at the bottom of a sterically restricted, hydrophobic cleft <8 Å wide at the top and >3 Å wide at the bottom, while the anionic center in the EA conformer is relatively open. It is characterized by a decrease in the relative binding of hydrophobic cations and by an ability to bind large organic cations. Binding of acetylcholine, H^+, or organic cations at the anionic site controls $k_{2(acylation)}$ in the E conformer and $k_{3(hydrolysis)}$ in the EA conformer. Acetylcholine binding forms the ES complex in which the cation maximizes k_2. In the EAS complex, the cation reduces k_3 and provides allosteric control. Anionic site structure and biochemistry and the effect of pH on k_2 and k_3 differentiates AChE from butyrlcholinesterase. This comprehensive study of kinetic and thermodynamic processes in AChE was made possible by the synthesis and/or use of families of over 30 cationic and acylation probes of known stereochemistry. They act as rulers of the E and EA conformers of AChE and provide comparative data on kinetic-based and thermodynamic-based constants. Cationic inhibitors affect decarbamylation rates in AChE and provide an additional set of comparative data related to the mechanism of substrate hydrolysis by AChE. Acridine araphanes are unique neural receptor and cholinergic enzyme probes. Their parallel plane and coplanar conformations are related to bridge length. Two parallel plane acridine araphanes are pure uncompetitive inhibitors of AChE. Scatchard plots of the binding of methylacridinium and 9-aminoacridine with the E conformer and 9-aminoacridine with the EA conformer indicate binding at a single anionic site. No ternary complex (EII or EAII) from two-site binding was detected. In AChE, nonspecific, low-level binding at surface ionic and hydrophobic areas is ubiquitous. Binding affinity differences greater than two orders of magnitude distinguish binding at the anionic site from low level binding at surface moieties. Surface binding provides environmental and stability changes in the enzyme but does not modify the fundamental biochemistry of the E and EA conformers.

AChE is an allosteric enzyme whose turnover number for ACh hydrolysis is $>10^4$ s^{-1} (1), among the highest reported for enzyme catalysis (2). As an allosteric enzyme, excess substrate inhibits the rate of hydrolysis. On a rate and biochemical basis, AChE is a unique hydrolytic enzyme. It has been described as an "evolutionarily perfect enzyme" (2).

Hydrolysis of ACh proceeds stepwise; the acetylated enzyme is an intermediate (3, 4). A change in structure of the anionic cleft accompanies acylation to produce EA (5). Any subsequent binding of an organic cation must then form an acylated enzyme-organic cation complex (EAS or EAI). The hydrolysis rate of the EAS and EAI complexes is low and may be zero. Most reversible cationic inhibitors show competitive (K_{d_1}) and uncompetitive (K_{d_2}), *i.e.*, "mixed" inhibition (5–7). Kinetics alone cannot distinguish whether K_{d_2} stems from binding at a

This work was supported in part by grants from the National Institutes of Health (grants NS 12471, NS 16478 to C.M.H.).

Mention of a trademark, warranty, proprietary product, or vendor does not constitute a guarantee by the U.S. Department of Agriculture and does not imply its approval to the exclusion of other products or vendors that may also be suitable.

[1] Presently retired.

ABBREVIATIONS: ACh, acetylcholine; AChE, acetylcholinesterase (E.C.3.1.1.7); BSA, bovine serum albumin; ChE, butyrlcholinesterase (E.C.3.1.1.8); E, free enzyme; EA, acylated enzyme; EI, enzyme inhibited by a cationic, reversible inhibitor; EAI, acylated enzyme inhibited by a cationic, reversible inhibitor; K_{D_1}, free enzyme (E) dissociation constant based on thermodynamic processes; K_{D_2}, acylated enzyme (EA) dissociation constant based on thermodynamic processes; $K_{d_{1,2}}$, enzyme-inhibitor dissociation constants obtained by kinetic processes; $K_{d_{50}}$, organic cation inhibitor concentration at 50% reduction in the decarbamylation rate of EA, numerically equal to K_D, the dissociation constant from binding of I with EA to give EAI; Maretin, *O,O*-diethyl-*O*-(1,6-naphthaloximido)phosphate; NMA, *N*-methylacridinium; 1–2E, 1–2-ethane-bis-9,9′aminoacridine; 1–2P, 1–2-propane-bis-9,9′aminoacridine; 9AA, 9-aminoacridine; NMR, nuclear magnetic resonance.

peripheral rate controlling site that exists on the free enzyme (noncompetitive) or from binding to: (a) a modified anionic site within the anionic center or (b) binding to a peripheral site, created on the EA conformer but not present in the E conformer. The latter two possible options characterize uncompetitive inhibition. Mechanisms for the regulatory control of AChE have been postulated (5, 8–10). These mechanisms assume that the kinetic (K_{d_2}) represents either noncompetitive or uncompetitive binding.

New probe systems with known stereochemistry can provide new information as to the nature of the anionic site present in the free and acylated enzyme conformers. We report the use of eight diverse families of more than 30 cholinergic probes with AChE and ChE. Comparison of equilibria, measured by kinetic-based and thermodynamic-based processes, provides new insight into the mechanism of substrate hydrolysis and allosteric control. Polyacene heterocyclic probes, having definable spectral effects and stereochemistry, have a singular value in fundamental studies of AChE. They have been used in studies of cholinergic enzymes in these and previously reported studies (5, 11–14).

This article provides data on the synthesis, kinetics, binding, and spectral properties of polyacene probes used in our research. It extends data on acridine araphanes (5, 14) and probes the intersite distance in the E and EA conformers. Inter- and intrafamily probe effects were compared under standardized conditions.

The research of Albuquerque and associates has shown that acridine araphanes, 9AA and 9-alkylaminoacridines, are new, valuable tools for the study of the nicotinic and muscarinic cholinergic receptors and the glutamate receptor (15–20). Recent data on the crystal structure of AChE have become available (21). Thus, structural data from x-ray crystallography can now be compared with structural data measured during the dynamic interactions of families of probes with AChE in solution.

We describe kinetic and binding data for two acridine araphanes that are structurally and chemically unique. They have been shown to be pure uncompetitive inhibitors of AChE.

Materials and Methods

AChE purification. AChE was obtained from frozen electric organ tissue of *Electrophorus electricus* by a simplified modification of Christopher *et al.* (22) using unquaternized 9AA as the affinity ligand (23). The combined 11-S tetramer fractions had a protein concentration of 0.5 mg/ml (by UV absorbance). Pooled 9.5 S, 14-S, and 18-S molecular forms had a protein concentration of 0.3 mg/ml. Probes were compared using pure 11-S AChE and the pooled molecular forms of AChE.

Normality of AChE solutions. Normality of AChE solutions was determined using the fluorescent organophosphate normality reagent Maretin (13; Molecular Probes, Bend, OR). Maretin has a known hydrolysis rate and pH profile and a well-defined phosphorylation rate, and is the only fluorescent acylation reagent whose leaving group is nonfluorescent and nonbinding at analytically significant levels (13).

Stability of AChE. Concentrated AChE was stable when frozen in high ionic strength buffer (I = 1.1). The buffer contained 1 M NaCl, 20 mM $MgCl_2$, and 10 mM total sodium phosphate (pH 7.5), plus 3 mM sodium azide. Low ionic strength buffer (I = 0.3) was prepared from 0.05 M sodium phosphate with 3 mM sodium azide and 0.5 mg/ml BSA.

Purified 11-S AChE and the heterogenous AChE fraction from affinity chromatography were stable over a 20-day period at 5° at both 6 and 12 × 10^{-9} N, even in low ionic strength buffer. The presence of 0.5 mg/ml BSA was critical for extended stability. Stability against bacterial action required 3 mM sodium azide in solutions stored over 5 days. Temperatures during kinetic and spectroscopic analyses were rigidly controlled. AChE was temperature equilibrated before use.

AChE activity, inhibition, binding, and kinetics. Probe-substrate-AChE interaction was measured by the Ellman method (24) and compared with data from the pH-stat method (25). Lineweaver-Burk inhibition plots were constructed using up to six inhibitor concentrations with data averaged from multiple (up to 20) repetitive runs. Steady state kinetics occurred below the substrate inhibition level (0.15 mM acetylthiocholine). Pure uncompetitive kinetics with 1–2E and 1–2P were verified by repetitive tests under standardized conditions of temperature, substrate level, enzyme normality, and reagent purity.

When the kinetic data from probe-substrate-AChE interactions showed mixed (competitive-uncompetitive) inhibition, the kinetic-based dissociation constants, K_{d_1} and K_{d_2}, were obtained using secondary replots of Lineweaver-Burk data. Slopes and y intercepts were obtained from least squares regression analysis.

The thermodynamic-based dissociation constant was determined by fluorescence quenching (26) of 9AA and NMA during titration of the E and EA conformers. The number of anionic sites in the E and EA conformers was determined by Scatchard plots. The probe of choice was 9AA. It is not subject to oxygen quenching.

Binding data were obtained using a Perkin Elmer 650–40 fluorescence spectrophotometer with digital output and full dynamic range. Scatchard plots for dual site binding were computer modeled. At the experimental conditions used, binding at a second anionic site could be detected if its $K_{D_{ss}}$ was within two orders of magnitude of the binding (K_{D_1}) at any primary site. In a preliminary communication (27), a two-site Scatchard plot was reported. Intensive reinvestigation showed that result to be an instrumental artifact from use of limited dynamic range sensitivity in an analog output spectrofluorometer; consequently, we use a digital output, full dynamic range instrument.

E and EA conformer binding with cationic inhibitors. Phosphorylated enzyme was formed by the reaction of Maretin with AChE (14, 26). *N*-Methycarbamyl, methylsulfonyl, and *N*,*N*-dimethylcarbamyl enzymes were prepared from the respective chlorides. Steric effects under dynamic conditions were studied with reversible cationic inhibitors at the anionic site during acylation of E, decarbamylation of EA, and binding to EA. The size of the acyl moiety affects these dynamics and measures the anionic-esteratic intersite distance in EA relative to E.

$K_{d_{60}}$ and K_{D_2} in carbamylated AChE. The *N*-methylcarbamylated enzyme was a valuable research system. Molecular models indicate that the *N*-methylcarbamoyl moiety is slightly larger than the acetyl moiety. Size of the acyl moiety increases in the order: acetyl, *N*-methylcarbamoyl, *N*,*N*-dimethylcarbamoyl, methylsulfonyl, diethylphosphoryl. The half-life of hydrolysis for the *N*-methylcarbamylated enzyme (and the *N*,*N*-dimethylcarbamylated enzyme) is sufficient to allow measurement of fluorescent probe binding. The kinetic rate of decarbamylation of EA was measured in the presence and absence of organic cationic inhibitors. Carbamylation of AChE reaches a maximum rate at pH 5.2; while at this pH, the rate of decarbamylation approaches zero. Decarbamylation rates were obtained from aliquots of the carbamylated enzyme (10^{-6} M), diluted by addition to cuvettes (pH 7) containing known concentrations of organic cation. After specific time periods, analysis for free AChE was made by the Ellman method. Recarbamylation and leaving group Cl^- were not analytically significant. Scatchard binding of 9AA with carbamylated enzyme was based on fluorescence quenching (26).

Analytical systems. The structures of the various probe ligands were confirmed by their proton NMR spectra (Varian HA-100) and ^{13}C NMR spectra (JEOL, gated 1 mode) using D_6-dimethylsulfoxide as the solvent with tetramethylsilane as the reference. The purity of all ligands was confirmed by high performance liquid chromatography analysis (C_{18} reverse phase, methanol-water + 1% acetic acid as solvent, methanol content was varied relative to the hydrophobicity of the probe) and elemental analyses. Corrected fluorescence spectra were obtained

using a Perkin Elmer model 650–40 fluorescence spectrophotometer. Quantum yields were determined by the relative method using quinine sulfate in 0.1 N H_2SO_4 ($\Phi = 0.55$) (26). Fluorescence spectra of ligands were obtained at 20° in absolute methanol or in aqueous, low ionic strength buffer. All probes were checked for oxygen quenching.

Probe synthesis. Pyridine and quinoline were dried over solid NaOH, decanted, distilled, and stored over molecular sieves. The dry, purified heterocycle was dissolved in benzene in the presence of excess alkyl iodide. Crystalline product was recovered after 12 hr at room temperature and recrystallized from acetonitrile. The quaternary salts of acridine were prepared using an excess of the appropriate 1-*n*-alkyl iodide in a sealed bottle at 40°. The *N*-methyl, *N*-ethyl *N*-propyl, and *N*-butyl quaternaries were filtered after 40–60 days, recrystallized from dry methanol, and purified by 2-day Soxhlet extraction using diethyl-ether to remove coprecipitated acridine. *N*-Methyl-9AA was prepared similarly using a 24-hr reaction period. 9AA and acridine were from Aldrich (Milwaukee, WI). They were recrystallized from 70% ethanol-water and from acetone. Edrophonium chloride was a gift from Hoffmann-LaRoche Inc. (Nutley, NJ).

9-*N*-Alkylaminoacridines and acridine araphanes were prepared by a modification of the method of Canellakis *et al.* (28). Water-miscible alkylamines were used in a 2–3 molar excess over 9-chloroacridine. Water-immiscible alkylamines were used in a 0.95 molar ratio with 9-chloroacridine. Acridine araphanes were prepared similarly using a 0.95 (equivalent) ratio of alkylene diamine to 9-chloroacridine. In all cases, the 9-chloroacridine was added in small amounts, over a 15-min period, to the stirred amine/phenol reaction mixture. Temperature was controlled to 60° and the reaction was maintained for 1 hr in a pure, dry nitrogen atmosphere. Phenol and acridone were removed by stirring the reaction product into a mixture of 200 ml $CHCl_3$, 400 ml ice, and 200 ml of solution that contained NaOH equivalent to the amount of phenol used. The cold $CHCl_3$ layer was washed to neutrality and dried, and then the $CHCl_3$ was removed *in vacuo*. The product was recrystallized from acetonitrile. Purity of all probes was determined by high performance liquid chromatography analysis.

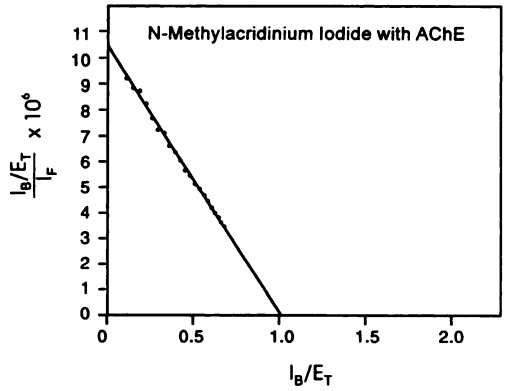

Fig. 1. Scatchard plot for the binding of NMA with AChE. Conditions: 10^{-6} M enzyme, incremental of NMA, T = 20°, monitored by the fluorescence quenching method (26). I_B = Inhibitor bound (quenched); I_F = inhibitor free (fluorescent); E_T = total enzyme (normality).

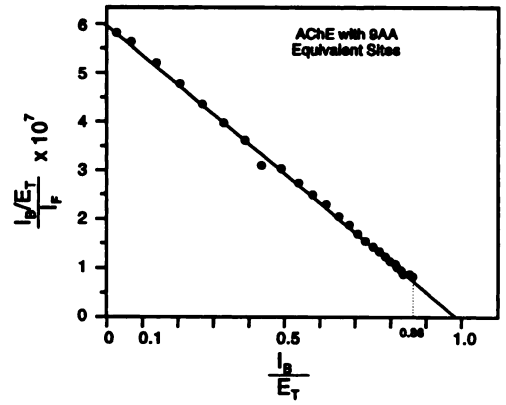

Fig. 2. Scatchard plot for the binding of 9AA with AChE. Conditions: 10^{-6} M enzyme, incremental addition of 9AA, T = 20°, monitored by the fluorescence quenching method (26), 9AA, excitation wavelength 400 nm, emission wavelength 435 nm.

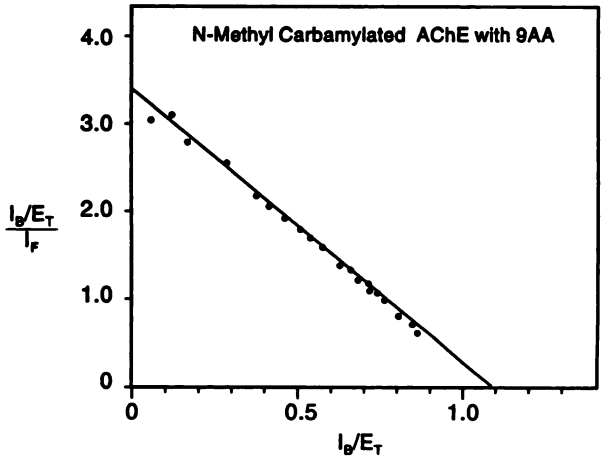

Fig. 3. Scatchard plot for the binding of 9AA with *N*-methylcarbamylated AChE. Conditions: 10^{-6} M enzyme, incremental addition of 9AA, T = 20°, monitored by the fluorescence quenching method (26), 9AA, excitation wavelength 400 nm, emission wavelength 435 nm.

Purified horse serum cholinesterase (ChE). Purified, stable horse serum cholinesterase was a gift from the late Professor A. R. Main.

Results

Purified, stable AChE and ChE were used for binding and kinetic studies with families of over 30 cationic or acylation probes. There is substantial value in the use of large numbers and families of probes in that intra- and interfamily effects can be compared. They show that AChE exists as E and EA conformers that differ in anionic site structure and biochemistry.

Binding of NMA and 9AA with the E conformer and 9AA with the EA conformer is shown in Scatchard plots (Figs. 1–3) based on the fluorescence quenching method (26, 29). A single, analytically significant anionic site is present in these conformers. They confirm the results of Mooser *et al.* (29) for binding of NMA with the free enzyme. The fully functional anionic site in the E and EA conformers is differentiated from ubiquitous surface anionic sites which are nonspecific and characterized by low levels of binding affinity.

In Table 1, using 9AA as inhibitor, kinetic-based binding constants are compared with thermodynamic-based binding constants. In the E conformer, K_{d_1} and K_{D_1} are equal. In the EA conformer, K_{d_2} has a value within the range of the K_{D_2} from binding with the *N*-methylcarbamylated, methylsulfonylated, and diethylphosphorylated enzyme. Binding to acyl enzyme reflects steric factors as a function of size of the acyl moiety. The data in Table 1 are significant in evaluation of the kinetics of AChE hydrolysis.

The architecture of the anionic site in both conformers was measured by two parallel plane (13) acridine araphanes 1–2E and 1–2P (Table 2, compounds 2A, 2B), whose structures are shown in Fig. 4. They are pure uncompetitive inhibitors of AChE (Fig. 5); thus, they do not bind within the cleft of the E

TABLE 1

Acetylcholinesterase/9AA kinetic-based and thermodynamic-based binding constants ($\times 10^{-7}$ M; pH = 7)

The Ellman method was used for kinetic data. The kinetic Kd_1 and Kd_2 values for a wide range of AChE probes are presented in Table 5. In general, Kd_2 represents a proximate 50% lesser binding at the opened and altered acylated conformer. Binding equilibria were obtained as indicated in Figs. 1–3.

Inhibitor	E Conformer		EA Conformer	
	K_{d_1} Kinetic	K_{D_1} Binding	K_{d_2} Kinetic	K_{D_2} Binding
9AA	0.25 ± 0.02	0.17 ± 0.05	0.52 ± 0.09	0.31 ± 0.08[a] 0.75 ± 0.45[b] 1.3 ± 0.35[c]

[a] From Scatchard plot, binding with *N*-methylcarbamylated AChE.
[b] From Scatchard plot, binding with methylsulfonylated AChE.
[c] From Scatchard plot, binding with diethylphosphorylated AChE.
[d] Reflects the effect of dynamic steric factors related to the size of the acyl moiety.

conformer. It is the three-dimensional structure of parallel plane acridine araphanes that prohibits their binding within the restrictive architecture of the anionic site in the free enzyme and which acts as a ruler to measure the cleft width at its top to be ≤8–9 Å. The bottom of this cleft is ≥3 Å, measured by binding and kinetic data from 9AA, 9-alkylaminoacridines, and *N*-alkylacridiniums (Tables 1, 3–5; Figs. 1 and 2). Based on these data, we suggest the architecture as shown in Fig. 6.

When there is no change in the anionic-esteratic intersite distance, pure uncompetitive kinetics (Fig. 5) indicate that 1–2E and 1–2P bind only within the altered anionic cleft of the EA conformer. That unique, specific binding is possible only because the anionic cleft in the EA conformer has less steric restrictions than the cleft in the E conformer.

Acetylation (acylation) of free AChE modifies the anionic site not only by opening of the cleft but also by change in biochemistry. AChE is also unique in that the anionic site is the focus of rate control mechanisms, controlling $k_{2(\text{acylation})}$ in the E conformer and $k_{3(\text{hydrolysis})}$ in the EA conformer. Rate control in each conformer is cation sensitive, thus binding of ACh to E gives ES, which controls k_2, and to EA gives EAS, which controls k_3.

Inhibition of AChE with NMA (and most cationic inhibitors) follows mixed, *i.e.*, competitive-uncompetitive kinetics (Fig. 7). Steric effects on the reaction dynamics during acylation and binding in the presence of 9AA and NMA provide comparative data on the anionic-esteratic intersite distance. On the basis of steric overlap effects (30), we suggest that this intersite distance does not change during acylation.

Unlike AChE, ChE shows competitive inhibition by 1–2P and 1–2E, which indicates that this cholinergic enzyme has an open configuration in its anionic center, analogous to the EA conformer of AChE. As noted previously, NMA is a competitive inhibitor of ChE (26) and is competitive-uncompetitive with AChE (Fig. 7).

9AA has been shown to be a significant new research tool in the study of cholinergic enzymes. It is photolytically stable, is not subject to oxygen quenching, and has a fluorescence quantum yield ($\Phi = 1$). Its maxima (λ_{max}, excitation wavelength 400 nm, emission wavelength 435 nm) are favorable for photolytic stability of AChE. Compared with NMA, it has 33% greater quantum yield and shows a 6- to 7-fold increase in binding affinity with AChE. Scatchard plots of NMA and 9AA with AChE show the significant analytical potential of 9AA (Figs. 1 and 2). 9AA provides viable analytical data even at the 90% binding range, well beyond that available with NMA.

The Scatchard plots in Figs. 1 and 2 are straight lines confirming the presence of a single binding site. The Scatchard plot for binding of 9AA with carbamylated AChE (EA conformer) is also a straight line (Fig. 3). If an analytically significant (and biochemically significant) peripheral anionic site were to be present on either the free or acylated enzyme, it would be reflected in a curved Scatchard line.

Theoretical effects of two-site binding in Scatchard plots

TABLE 2

Physical properties of acridine araphanes[a]

No.	Name	M.P.	Interplane distance	Fluorescence λ		Quantum yield	Inhibition kinetics
				Ex_{max}	Em_{max}		
		°	Å	nm			
2A	1-2,Ethane-bis-9,9′-aminoacridine	234–235	3.5	—[b]	—[b]	—[b]	—[c]
2B	1-2,Propane-bis-9,9′-aminoacridine	204–205	3.5	—[b]	—[b]	—[b]	—[c]
2C	1-3-Propane-bis-9,9′-aminoacridine	198–199	5.0	410	487 466s	0.003	Mixed
2D	1-4-*n*-Butane-bis-9,9′-aminoacridine	203–204	6.1	414 466s	485	0.006	Mixed
2E	1-5-*n*-Pentane-bis-9,9′-aminoacridine	191–192	7.3	ND[d]		ND	Mixed
2F	1-6-*n*-Hexane-bis-9,9′-aminoacridine	181–182	8.5	412	486	0.009	Mixed
2G	1-7-*n*-Heptane-bis-9,9′-aminoacridine	173–174	9.8	ND		ND	ND
2H	1-9-*n*-Nonane-bis-9,9′-aminoacridine	178–179	12.0	ND		ND	ND
2I	9-*n*-Propyl-aminoacridine[e]	98–99		413	486	0.016	Mixed

[a] Ex, excitation wavelength; Em, emission wavelength; s, shoulder.
[b] Nonfluorescent.
[c] Pure competitive.
[d] ND, not determined.
[e] Compound 2I shows typical ranges for fluorescence data for 9-*n*-alkylaminoacridines.

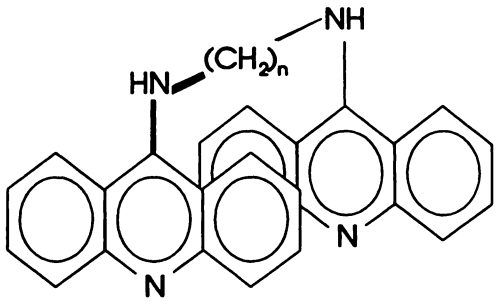

Fig. 4. Parallel plane acridine araphanes.

were investigated by computer modeling of binding equilibria for the enzyme-inhibitor complexes EI, EI', and EII', and, in the acylated enzyme, inhibitor complexes EAI, EAI', and EAII'. Two analytical criteria were modeled: (a) probe quenching at both binding sites; and (b) probe quenching with only the EI or EAI complex.

In case 1, with two-site binding and quenching, the computer-generated Scatchard plot was a *curved* line from the origin to two binding sites. In case 2, with two-site binding but fluorescence quenching at only one site, the Scatchard plot was also a *curved* line from the origin to one binding site. A wide range of relative binding constants was used in the calculations, including K_{d_1} and K_{d_2} (Table 5) and up to two orders of magnitude variation. We conclude that the single-site, straight-line Scatchard plots (Figs. 1–3) are strong evidence that a single anionic site exists in the E and EA conformers of AChE, *i.e.*, there is no analytical evidence for a biochemically significant peripheral anionic site in AChE.

Acridine Araphanes

Acridine araphanes are new probes of neural receptors (15–20) and AChE (14). Data on this probe series are given in Tables 2 and 3. The parallel plane conformation was defined by proton NMR chemical shift data and verified by ^{13}C coupled spectra (14). The parallel plane conformation exists even in dilute solution. Their UV-Vis absorption spectra (Fig. 8) and extinction coefficients (Table 3) provide additional confirmation. Parallel plane acridine araphanes represent a chemically unique molecular conformation that is the stereochemical equivalent of a stable, three-sided box. That stability (in the absence of a cyclophane-type covalent bond) stems from transannular effects (π-electron overlap) when the two acridine rings are in close juxtaposition. These attractive forces are similar to those which are the basis of eximer fluorescence in concentration dimers and in the phenomenon of stacking of aromatic moieties in concentrated solution. Parallel plane acridine araphanes are unique in that they are stable in the parallel conformation even in dilute solution and in a wide range of solvents.

The study of the effect of cationic inhibitors on the rates of decarbamylation of *N*-methylcarbamylated AChE was helpful in interpretation of AChE kinetics. For each specific cationic inhibitor, the inhibitor concentration producing 50% reduction of the decarbamylation rate ($K_{d_{50}}$) was found to be numerically equal to K_{D_2} and its uncompetitive inhibition constant (K_{d_2}). This is substantial evidence that in the kinetics of ACh hydrolysis, $k_{3(\text{hydrolysis})}$ is a key factor in K_{d_2}, and that for the complex EAI and EAS, k_3 is zero.

Other Probes, Including Acridines, Quinolines, and Pyridines

A wide range of cationic probes other than acridine araphanes were synthesized or used in this study. For convenience, they are listed in Table 4, with identification number, name, and melting point (if applicable). Numbers in this table identify these probes in subsequent tables and in the text. Data on the kinetics of acridine, quinoline, pyridine, and their derivatives are presented in Table 5. Many probes in Table 5 act as rulers for the structure of the anionic cleft in the E and EA conformers, as suggested in Fig. 6. Table 5 also provides binding data for edrophonium and tetramethylammonium. Edrophonium binds to both the anionic and esteratic sites and is a competitive inhibitor of AChE (Fig. 9).

The Anionic Center in the E Conformer of AChE

The anionic site has been proposed to be a trimethyl binding site (31) and one in which the hydrophobic nature of the walls of the cleft are of major significance (21). The trimethyl site was rejected in a recent review (2) citing experimental data (32). Binding data in Table 5 support the existence of an anionic

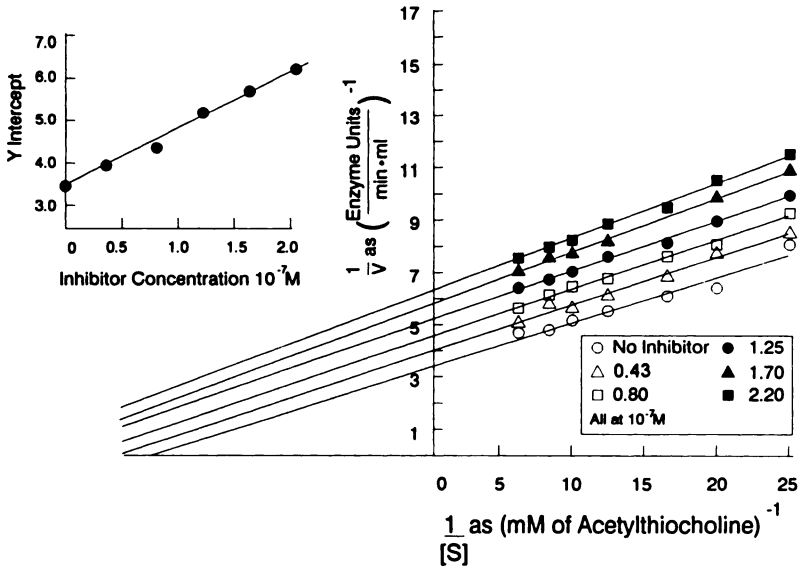

Fig. 5. The pure uncompetitive kinetics of inhibition of AChE by 1–2E. Lineweaver-Burk plot of inhibition with pure 11-S AChE. Data were obtained by the Ellman method at pH 7 and ionic strength 0.3. Secondary plots are shown as inserts. All lines were fitted by least squares regression analysis.

TABLE 3

UV-Vis absorption data for acridine araphanes in methanol

Compound (2I) represents 9-*n*-propylaminoacridine and is characteristic of the absorption spectra for 9-alkylaminoacridines that have a single chromophore. The acridine araphane extinction coefficients reflect the presence of two separate chromophores. Spectra are given in Fig. 8. s, shoulder.

Cpd no.	λ_{max}	ϵ	λ_{max}	ϵ	λ_{max}	ϵ	λ_{max}	ϵ
	nm		*nm*		*nm*		*nm*	
2A	259	89,500	396	13,900			433	7,800
2B	260	91,100	397	13,100			435	7,800
2C	259	98,500	396	14,900	407	14,700	433	8,000
2D	263	101,000	394	15,100	410	18,700	433	13,700
2F	267	108,100	393s	14,600	411	20,700	433	15,900
2I	268	60,800	392s	7,400	410	11,000	432	9,000

TABLE 4

Probes from 9AA, acridine, quinoline, and pyridine

All probes were purified to the level of a single peak when analyzed by high performance liquid chromatography (C_{18} reverse phase, methanol-water + 1% acetic acid as solvent). All were synthesized, except for 4O (from Hoffmann-La Roche) and 4J and 4P through $4Q_3$ (purchased from Aldrich). Acridine araphane probes are given in Table 2 while their related 9-alkylaminoacridine, acridinium, quinolinium, and pyridinium probes are tabulated above. Many of these probes have useful spectral activity in addition to their cholinergic activity. Quaternary probes and the tertiary heterocyclic 9AA, 9-alkylaminoacridine, and acridine araphanes all have pK_a values in the range of 9.5 to 11. Acridine, quinoline, and pyridine ($4Q_1$-$4Q_3$) have pK_a values in the range of 5 to 6.

Probe no.	Name	Melting point
		°C
4A	9-*n*-Propylaminocridine	98–99
4B	9-*n*-Butylaminoacridine	103–104
4C	9-*n*-Isobutylaminoacridine	145–146
4D	9-*n*-Pentylaminoacridine	100–102
4E	9-*n*-Octylaminoacridine	87–88
4F	*N*-Methylacridinium iodide	228–230
4G	*N*-Ethylacridinium iodide	226–227
4H	*N*-*n*-Propylacridinium iodide	219–221
4I	*N*-*n*-Butylacridinium iodide	212–214
4J	9-Aminoacridine	232–233
4K	9-Amino-10-methylacridium iodide	>300
4L	*N*-Methylquinolinium iodide	135–136
4M	*N*-*n*-Butylquinolinium iodide	174–175
4N	*N*-Methylpyridinium iodide	112–114
4O	Edrophonium chloride	162–163
4P	Tetramethylammonium bromide	
$4Q_1$	Quinoline	
$4Q_2$	Acridine	
$4Q_3$	Pyridine	

center and indicate that the anionic center is the focus of rate control within AChE. The data define its location and describe the architecture of the anionic cleft as suggested in Fig. 6. Data are discussed below.

Relative binding of pyridine, quinoline, acridine, and their *N*-methyl quaternaries. The anionic site binding of pyridine ($4Q_3$, $105{,}000 \times 10^{-7}$ M), quinoline ($4Q_1$, 4, 300×10^{-7} M), and acridine ($4Q_2$, 332×10^{-7} M) are increased 200-, 80-, and 240-fold, respectively, when converted to their *N*-methyl quaternaries (4N, 506×10^{-7} M; 4L, 56×10^{-7} M; 4F, 1.4×10^{-7} M). Within these three heterocyclic acene ring systems, binding affinity increases as the pKa (cationic strength) increases and as hydrophobicity increases.

Relative binding of 9AA and its *N*-methyl quaternary. The relative binding of 9AA (4J) and its quaternary 9-amino-10-methylacridinium (4K) is significant. The quaternary had increased hydrophobicity and increased cationic strength (pKa 11.18 versus 9.99), yet its binding to AChE was 80% less than that of 9AA. This decrease shows cation-anion (coulombic) charge separation caused by the steric size of the methyl moiety acting within the architecture of the anionic cleft. Because quaternization of 9AA decreased binding to AChE, a simplified, nonquaternary 9AA affinity chromatography ligand was developed for purification of AChE (23). These data suggest that an anionic center exists at or close to the bottom of the cleft but does not lie in a "pocket" below the bottom of the cleft (2, 21).

Relative binding of *N*-alkylacridiniums and *N*-alkylquinoliniums. Steric and charge separation effects are found in the relative binding of *N*-alkylacridinium probes. In general, binding decreased as the steric size of the alkyl quaternary was increased from methyl (4F) to ethyl (4G) to *n*-propyl (4H) and to *n*-butyl (4I). The steric effect of the alkyl moiety decreased overall binding of the alkyl quaternary probe (Table 5).

Quinolinium probes, on the other hand, can bind with the quaternary alkyl moiety under the benzo ring or away from the heterocyclic ring. In the latter conformation, steric effects would be limited. *N*-*n*-Butylquinolinium (4M) binds 1.4-fold stronger than *N*-methylquinolinium (4L), reflecting increased hydrophobic binding of the butyl group and minimal steric effects (Table 5).

Binding conformations of 9AA and 9-alkylaminoacridines within the anionic cleft. 9AA and its 9-alkyl analog confirm the presence of an anionic center in AChE. If there were no anionic center, then 9AA and 9-*N*-*n*-pentylacridine (4D) could bind within the cleft with the 9-NH_2 and 9-*N*-*n*-pentyl moieties at the bottom of the cleft. With these probes in that conformation, the binding would be in the range of that of acridine ($4Q_2$). Their binding is three orders of magnitude greater than acridine, indicating that they bind with the hetero N (pKa 9–10) at the bottom of the cleft (Table 5).

Stereochemistry of the Anionic Site of the E Conformer

The width of the anionic cleft is ≤8–9 Å, measured by the kinetics of the acridine araphanes 1–2E and 1–2P (compounds 2A and 2B in Table 2), which have a molecular width of 8–9 Å. As pure, uncompetitive inhibitors of AChE (Fig. 5), they do not bind at the anionic site of E, providing a measure of the width of the anionic cleft at its top. Since 9AA binds at the bottom of the anionic cleft, it defines a minimum width for that area of 3 Å. The proposed architecture for the anionic cleft in AChE is illustrated in Fig. 6.

Stereochemistry of the Anionic Site of the EA Conformer

K_{d_2} and K_{D_2} measure binding of cationic inhibitors at the anionic center of the EA conformer. Any proposed architecture for this site must accommodate the fact that probe binding in this conformer is less than that measured by K_{d_1} and K_{D_1} in the E conformer. The open architecture for EA proposed in Fig. 6

TABLE 5

Binding parameters at the anionic site of AChE: binding of acridine series probes[a]

Dissociation constants are for the anionic (K_{d_1}) and allosteric (K_{d_2}) sites on AChE, with 95% confidence limits. The Ellman method (except as indicated) was used at 20° (ionic strength 0.3). Use of high ionic strength buffer (ionic strength 1.1) increased the rate of the reaction and decreased the binding of cationic inhibitors. The competitive-uncompetitive kinetics were not changed by ionic strength or molecular form (9.5-S, 14-S, 18-S) of the AChE. Data for selected probes analyzed by the pH-stat method (at pH 7) are included in this table. Consistent with the concept that the kinetic K_{d_2} measures the lower level of hydrophobic binding at an opened and altered acylated anionic site, K_{d_2} values reflect a proximate 50% lesser degree of binding in comparison with K_{d_1}.

No.	Probe	pH	K_{d_1}	K_{d_2}
			$\times 10^{-7}$ M	
4J[a]	9AA (pKa 9.99)[b]	5.7	0.25 ± 0.02	1.4 ± 0.08
		7.0	0.26 ± 0.02	0.52 ± 0.09
		8.1	0.17 ± 0.02	0.23 ± 0.02
	pH stat method	7.0	0.15 ± 0.04	0.41 ± 0.06
4D[a]	9-*n*-Pentylaminoacridine	5.7	1.81 ± 0.3	2.02 ± 0.4
		7.0	0.55 ± 0.3	2.23 ± 0.1
		8.1	0.78 ± 0.1	1.17 ± 0.3
4K[a]	9-Amino-10-methylacridinium (pKa 11.18)[c]	7.0	1.2 ± 0.3	5.0 ± 0.7
	pH stat method	7.0	1.2 ± 0.4	2.5 ± 0.8
4F[a]	NMA (pK_a 9.85)[c]	5.7	1.7 ± 0.2	3.6 ± 0.8
		7.0	1.4 ± 0.2	2.7 ± 0.3
		8.1	1.3 ± 0.1	2.1 ± 0.1
	pH stat method	7.0	1.0 ± 0.3	2.0 ± 0.8
$4Q_2$	Acridine (pK_a 5.6)[c]	8.1	332 ± 15	753 ± 25
4G	*N*-Ethylacridinium	7.0	1.8 ± 0.2	4.8 ± 0.2
		8.1	0.5 ± 0.9	5.1 ± 0.9
	pH stat method	7.0	1.8 ± 0.5	5.0 ± 2.4
4H	*N*-*n*-Propylacridinium	7.0	2.2 ± 0.1	5.5 ± 0.9
	pH stat method	7.0	2.7 ± 0.7	5.6 ± 2.1
4I	*N*-*n*-Butylacridinium	7.0	3.5 ± 0.3	6.8 ± 0.8
		8.1	3.1 ± 0.6	7.2 ± 0.6
	pH stat method	7.0	4.4 ± 1.5	8.7 ± 3.2
4L	*N*-Methylquinolinium	5.7	120 ± 27	506 ± 87
		7.0	56 ± 11	243 ± 61
		8.1	59 ± 30	153 ± 51
$4Q_1$	Quinoline	8.1	4,300 ± 200	10,000 ± 540
4M	*N*-*n*-Butylquinolinium	7.0	40 ± 7	120 ± 10
		8.1	41 ± 1	78 ± 4
4N	*N*-methylpyridinium	5.7	829 ± 80	
		7.0	506 ± 107	1,170 ± 200
		8.1	441 ± 83	924 ± 92
$4Q_3$	Pyridine	8.1	105,000 ± 402	
4O	Edrophonium	5.75	1.3 ± 0.5	
		7.0	0.6 ± 0.1	
4P	Tetramethylammonium	7.0	5,500 ± 129	
		8.1	5,700 ± 129	

[a] The first four probes (4J, 4D, 4K, 4F) provide data as to the existence of an anionic center and its location within the anionic cleft. Additional data in Table 5 provide confirmation.
[b] Reference 33.

is based on the binding of 1–2E and 1–2P at anionic sites of the EA conformer and decreased hydrophobic contribution to binding by reason of the open conformation (Tables 1, 2, and 5, Fig. 6).

Dynamic steric interference by cation probes occurred during acylation of the E conformer, during binding to the acylated enzyme, and during deacylation of *N*-methylcarbamylated or *N*,*N*-dimethylcarbamylated AChE. Steric overlap between 9AA (or NMA) and the phosphorylating agent Maretin were recognized by effects on the second order rate of phosphorylation (14) and by the slope of the Scatchard plot. The overlap effects in dynamic binding systems have been described (14, 26).

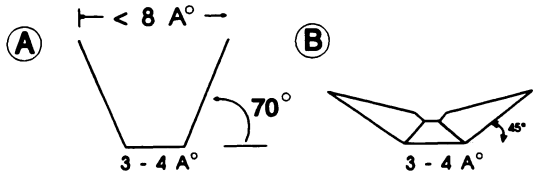

Fig. 6. End configuration of the anionic cleft in the E and EA conformers of AChE. The anionic cleft in the E conformer has a restrictive stereochemistry. It is <8–9 Å at the top and ≥3 Å at the bottom. The altered anionic cleft in the EA conformer binds parallel plane acridine araphanes and has minimal steric restrictions. The angle in the E conformer was estimated by the angle formed from a 3-Å bottom and an 8- to 9-Å top for the cleft. The angle in the EA conformer was estimated as less than that in the E conformer and greater than 0–15°.

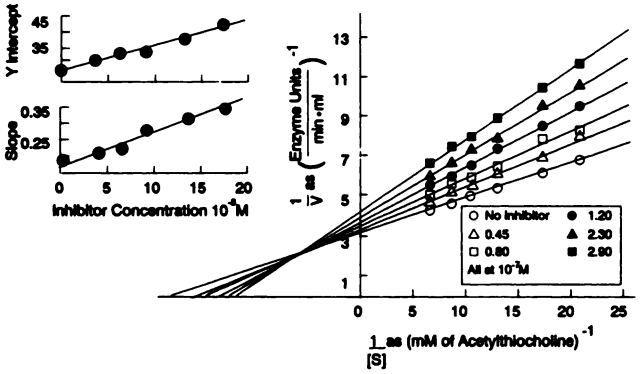

Fig. 7. The mixed kinetics of inhibition of AChE with NMA. Conditions are as described in Fig. 5.

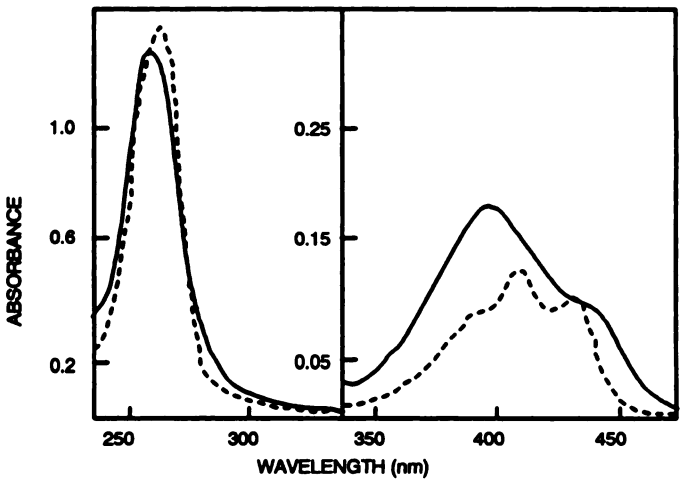

Fig. 8. UV-Vis spectra of acridine araphanes in methanol. In both water and methanol, the araphanes with a parallel plane conformation (solid line) have three distinct differences in their UV absorption spectra from the spectra of the related single ring system 9-alkylaminoacridines (broken line). The complex three-peak structure at 410 nm, which corresponds to the n-π transition, is lost to a broad single peak in the related parallel plane structure. The strongly absorbent π-π^* transition peak at 268 nm shows a progressively increasing hypsochromic shift with decreasing numbers of carbon atoms in the bridge. The shift of the π-π^* absorption is accompanied by a progressive decrease in extinction coefficient.

Maretin binds preferentially at a hydrophobic area adjacent to the esteratic site and not at the anionic site of AChE. Dynamics of binding of cationic probes of known size with the acylated enzyme reflect the anionic-esteratic intersite distance. Although steric constraints in the EA conformer are minimal,

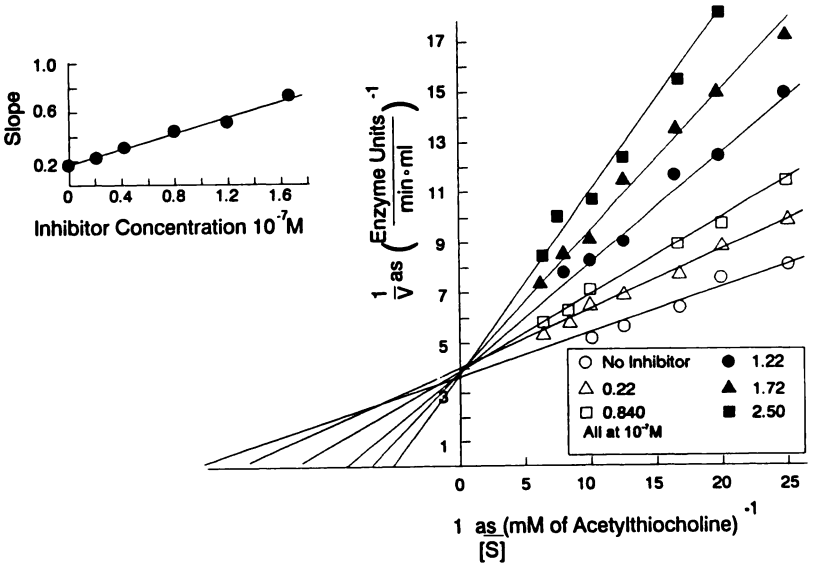

Fig. 9. The competitive kinetics of inhibition of AChE with edrophonium.

there are significant hydrophobic and charge separation effects, indicating that the cleft angle is >15°. The relatively open stereochemistry allows binding of large and polyfunctional cationic probes.

Overlap effects in the EA conformer occurred during the binding of 9AA and NMA with diethylphosphorylated AChE, with *N*,*N*-dimethylcarbamylated AChE, but not with *N*-methylcarbamylated AChE. The dynamic overlap effects in EA were not different from those in the E conformer, indicating that the anionic-esteratic intersite distances in the E and EA conformers are substantially the same.

Discussion

Cationic inhibitory ligands influence the steady state kinetics of AChE as competitive (Fig. 9), mixed or competitive-uncompetitive (Fig. 7), and pure uncompetitive (Fig. 5). Pure competitive kinetics results from the inhibitor (such as edrophonium) binding at both the anionic and esteratic sites of the E conformer. The majority of organic cation inhibitors show mixed inhibition of AChE. Pure uncompetitive kinetics are rare and appear to be unique to parallel plane acridine araphanes and similar three-dimensional, space-filling organic cations.

Kinetic data alone cannot resolve whether the competitive-uncompetitive (mixed) inhibition is uncompetitive or noncompetitive. We suggest that the data in this paper identify mixed kinetics as competitive-uncompetitive in which the uncompetitive component represents binding to the altered anionic cleft structure in the EA conformer.

In Table 1, the binding constant (K_{D_1}) for 9AA with AChE is the same as the kinetic K_{d_1}. Also in Table 1, the binding constant (K_{D_2}) for 9AA binding with the *N*-methylcarbamylated enzyme is experimentally equal to the kinetic K_{d_2}. We suggest that this is also good evidence the mixed inhibition is competitive-uncompetitive and not competitive-noncompetitive. As indicated previously, the K_{D_2} values are affected by the size of the acyl moiety relative to acetyl.

Scatchard plot data (Figs. 1–3) identify the presence of a single anionic site in the E and EA conformers of AChE. That single-site determination indicates that no EII or EAI complex can be found in the AChE system by NMA and 9AA. It is experimental evidence that no analytically significant peripheral anionic site is present and that mixed AChE inhibition kinetics are not noncompetitive. Pure uncompetitive inhibitors are rare, and their inhibition kinetics (in conjunction with other data) suggest that the uncompetitive component stems from binding of the cation at the "altered" anionic site of the EA conformer (Fig. 6).

Various models for the mechanism of action and regulatory control in AChE have been postulated. Over a period encompassing four decades, rate control through organic cation binding at a peripheral anionic site has gained status as conventional wisdom (34–37). Most organic cations described as peripheral anionic site probes are either large polyquaternaries or alkylene bridged bisquaternaries such as decamethonium, propidium, hexidium, or decidium. The site of binding of their ω-quaternary moiety is generally described as "peripheral" and "anionic." It is reasonable that such binding can be peripheral, but there are no rigorous spectroscopic or binding data that confirm any anionic nature to the peripheral site of binding. Such confirmation would include independent measurement of the degree of binding of organic cation probes at any EII or EAII binding site on AChE, a result that has not been met in the present or any publication. Spectroscopic data including fluorescence do not confirm binding of the ω-moiety at an anionic site either by quenching or by spectral shift data. Spectral shifts on binding of the phenanthridinium moiety are consistent with those expected from binding within hydrophobic areas.

Surface ionic and hydrophobic sites are ubiquitous on proteins, including AChE. They are characterized by very low binding levels relative to the binding of organic cations at the active center of the anionic site in AChE. We suggest that the ω-quaternary moiety in bisquaternaries binds at peripheral hydrophobic and/or surface ionic sites on AChE that have no critical rate control functionality.

We suggest that rate control in AChE is centered within the biochemistry of the anionic center of the E and EA conformers. This allows a simplified mechanism for the mechanism of action of AChE (Fig. 10). In Fig. 10, rate control of acylation (k_2) resides within the anionic site of the E conformer, while rate control of hydrolysis (k_3) resides within the anionic site of the EA conformer. Both k_2 and k_3 are pH *and* cation sensitive.

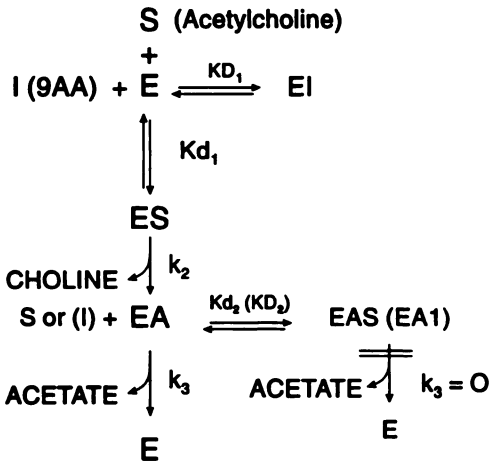

Fig. 10. Mechanism of action and regulatory control model for AChE.

Binding of the cationic substrate ACh to produce ES maximizes the rate of acetylation, while its binding to EA gives EAS whose k_3 is zero.

The first step of the mechanism involves binding of ACh. Binding within the sterically restricted anionic cleft produces the ES (Michaelis) complex and an induced-fit microconformer. In the presence of inhibitor, the process is measured by K_{d_1}. Binding of organic cations to E is measured by K_{D_1}. Binding in AChE is pH sensitive, decreasing between pH 8–5 (13).

The second step of the mechanism involves acetylation of AChE, with a concomitant opening of the anionic cleft to give the EA conformer and release of choline. Release of choline is expedited by its low binding affinity within the open structure of the anionic cleft. The acetylation process is measured by the kinetic rate constant k_2. Organic cations bind to the EA conformer to give the complex EAI, as measured by the thermodynamic dissociation constant K_{D_2}.

The hydrolysis of the EA conformer is the third step. It is measured by k_3 and is generally rate controlling. Its products are acetate ion and the free enzyme (E). In this allosteric enzyme, the hydrolysis rate of the EAS complex (k_3) is either low or zero. Equivalent values for K_{d_2}, K_{D_2}, and $K_{d_{50(deacetylation)}}$ suggest that k_3 is zero for hydrolysis of the complexes EAS and EAI.

The competitive nature of the binding of substrate and inhibitor, forming ES and EI, is reflected in equivalent values for K_{d_1} and K_{D_1}. In the EA conformer, K_{d_2}, K_{D_2}, and $K_{d_{50}}$ are also equivalent in value. In the E and EA conformers, kinetic-based and thermodynamic-based constants were found to have a common structural-biochemical basis. That common basis is significant in interpretation of AChE kinetics.

As indicated previously, two key biochemical rate mechanisms that are cation dependent regulate k_2 and k_3 in the E and EA conformers of AChE. Within the anionic site, rate control is centered within a radius of a few Å and regulates the ES, EA, EAS, EI, and EAI complexes. Highly focused rate control mechanisms within the anionic site, along with a serine-histidine-glutamate triad (21), illustrate the uniqueness of AChE.

In the free enzyme E, the anionic site lies at the bottom of a sterically restricted cleft. The bottom is flat, or substantially flat, and has no methyl pocket (2, 21). The walls of the cleft contribute a substantial hydrophobic contribution to the total binding of organic cations. The slope of the cleft walls aids in the entry, positioning, and optimization of the binding of ACh. The stereochemistry of the cleft and its depth limits the entry and/or binding effects of large, polyfunctional probes. The cleft dimensions readily accommodate the 9AA ring system and that of *N*-alkyl quaternary acridines. The affinity binding of organic cations reflects their stereochemistry, hydrophobic nature, and pKa.

All proteins, including AChE, owe the stability of their tertiary structure(s) to peripheral binding of ions and organic molecules. We found AChE to be stable over extended periods in high ionic strength media. That stability decreased as ionic strength decreased. Addition of BSA increased the stability of AChE by surface binding effects with the enzyme. Binding on the surface of AChE reflects the presence of hydrophobic, cationic, and anionic areas. These surface binding areas are characterized by their ubiquitous presence, nonspecificity of binding, and low level of binding relative to the anionic site binding of NMA and 9AA.

Binding of polyfunctional molecules reflects additive effects for each of their component structures. The contribution of surface ionic and hydrophobic binding in polyfunctional molecules has not been quantitated. Thus, their peripheral binding can have no structural implications. Nonspecific binding can determine the environment of AChE but has no key part in the biochemical rate control processes which are the province of binding within the anionic core of the enzyme.

This research is based on the interaction dynamics of active site-directed probes with AChE in solution. Data from these interactions can now be compared with data from x-ray crystallographic studies. In the AChE crystal, the anionic center is described as "a deep and narrow gorge" with hydrophobic amino acids in the walls (21). In solution, the E conformer has a deep and narrow cleft. The hydrophobic nature of the walls of the cleft was measured by binding data from the series tetramethylammonium, *N*-methylpyridinium, *N*-methylquinolinium, and *N*-methylacridinium. That binding increased 10-, 100-, and 4000-fold, respectively. The increase in the hydrophobic component of binding approximates an order of magnitude or more for each additional aromatic ring.

Hydrophobic binding can be selective. The hydrophobic phosphorylation probe Maretin bound preferentially at a hydrophobic area adjacent to the esteratic site, not within the anionic cleft. It formed a ternary complex, NMA-AChE-Maretin, the emission spectrum of which is identical to that of the AChE-Maretin complex. Maretin does not compete with NMA for the anionic site. The dynamics of Maretin phosphorylation show steric overlap effects with NMA.

Parallel plane and co-planar acridine araphanes are unusual new receptor probes. They are unique in their biological activity at the cholinergic (muscarinic and nicotinic) receptors and the glutamate receptor (15–20). They represent novel tools in the study of cholinergic neural transmission.

Unlike AChE, ChE has no allosteric mechanism. It has an open architecture in its anionic center since it reacts with 1–2E by a competitive inhibition mechanism. Significant differences exist in AChE and ChE active site biochemistry. That difference includes pH effects on Michaelis binding and on the rate of acylation. The rate of phosphorylation of ChE is essentially constant through the acid range, but affinity binding decreases on both sides of pH 7. In contrast, the rate of phosphorylation of AChE increases with a decrease in pH and binding decreases over the entire pH range from 8 to 5 (5, 13).

It has been reported previously that phosphorylation of AChE by diisopropyl fluorophosphate showed an increase in phosphorylation rate as pH decreased from 6 to 5 (38).

We believe that the design, synthesis, and use of diverse series and families of spectroscopic and stereochemical probes are significant in the study of kinetic and thermodynamic processes within the active site of AChE. They provide a contribution to fundamental knowledge of this enzyme.

Acknowledgments

This study is dedicated to the memory of Professor Carl S. Marvel, Department of Chemistry, University of Illinois.

References

1. Michel, H. O., and S. Krop. The reaction of cholinesterase with diisopropylfluorophosphate. *J. Biol. Chem.* **190**:119–125 (1951).
2. Quinn, D. M. Acetylcholinesterase: enzyme structure, reaction dynamics and virtual transition states. *Chem. Rev.* **87**:955–979 (1987).
3. Krupka, R. M., and K. J. Laidler. Molecular mechanisms for hydrolytic enzyme action. II. Inhibition of acetylcholinesterase by excess substrate. *J. Am. Chem. Soc.* **83**:1448 (1961).
4. Krupka, R. M. Acetylcholinesterase. *Can. J. Biochem. Physiol.* **42**:677 (1964).
5. Taylor, J. L. Acetylcholinesterase: the nature and mechanism of the active and regulatory sites. Ph.D. thesis, University of Georgia (1981).
6. Lineweaver, H., and D. Burk. The determination of enzyme dissociation constants. *J. Am. Chem. Soc.* **56**:658–670 (1934).
7. Rosenberry, T. L., and S. A. Bernhard. Studies of catalysis by acetylcholinesterase. Synergistic effects of inhibitors during the hydrolysis of acetic acid esters. *Biochemistry* **11(23)**:4308–4321 (1972).
8. Mooser, G., and D. Sigman. Ligand binding properties of acetylcholinesterase determined with fluorescent probes. *Biochemistry* **13(11)**:2299–2307 (1974).
9. Barnett, P., and T. L. Rosenberry. Catalysis of acetylcholinesterase. *J. Biol. Chem.* **252(20)**:7200–7206 (1977).
10. Main, A. R. Mode of action of anticholinesterases. *Pharmacol. Ther.* **6**:579–628 (1979).
11. Himel, C. M., R. T. Mayer, and L. L. Cook. Design of active-site-directed fluorescent probes and their reaction with biopolymers. *J. Polymer Sci. Pt A-1* **8**:2219–2230 (1970).
12. Himel, C. M., and L. M. Chan. Synthetic fluorescent substrate analog, in *Concepts in Biochemical Fluorescence* (R. Chen and H. Edelhoch, eds.), Vol. 2. Dekker, New York, 607–637 (1976).
13. Himel, C. M., and J. L. Taylor. Phosphorylation rate constant and esteratic subsite normality employing the fluorescent organophosphate Maretin: a new approach to the study of the acylation mechanism of acetylcholinesterase and butyrylcholinesterase. *Pest. Biochem. Physiol.* **17**:103–112 (1982).
14. Himel, C. M., J. L. Taylor, C. Pape, D. B. Millar, J. Christopher, and L. Kurlansik. Acridine araphanes: a new class of probe molecules for biological systems. *Science* **205**:1277–1279 (1979).
15. Silvera, F. C. A., M. E. Nelson, K. P. Shaw, R. S. Aronstam, and E. X. Albuquerque. A study of acridine analogs on nicotinic receptors. *FASEB J.* **4**:A470 (1990).
16. Shaw, K. P., F. C. A. Silvera, R. S. Aronstam, and E. X. Albuquerque. A new class of cholinergic antagonists. *Neurosci. Abstr.* **16**:1060 (1990).
17. Shaw, K. P., C. M. Himel, and E. X. Albuquerque. Acridine analogs block muscarinic receptors [Abstracts]. *FASEB J.* **4**:A471 (1990).
18. Shaw K. P., R. S. Aronstam, C. M. Himel, and E. X. Albuquerque. Acridine derivatives as new probes of muscarinic acetylcholine receptors (unpublished).
19. Shaw, K. P., S. Pou, R. S. Aronstam, C. M. Himel, P. S. Callery, and E. X. Albuquerque. Mapping of cholinergic receptors using acridine araphanes, a new class of potent antagonists (unpublished)
20. Shaw, K. P., F. C. A. Silverira, R. A. M. Reis, R. Rosenthal, E. F. R. Pereora, Y. Aracava, C. M. Himel, and E. X. Albuquerque. Tetrahydroaminoacridine and other acridines block the nicotinic acetylcholine receptor-ion channel complex (unpublished).
21. Sussman, J. L., M. Harel, F. Frolow, C. Oefner, A. Goldman, L. Toker, and I. Silman. Atomic structure of acetylcholinesterase from *Torpedo californica:* a prototypic acetylcholine-binding protein. *Science* **253**:872–879 (1991).
22. Christopher, J. P., L. Kurlansik, D. B. Millar, and C. Chignell. On the homogeneity of 11-S acetylcholinesterase. *Biochim. Biophys. Acta* **525**:112–123 (1978).
23. Taylor, J. L., W. K. Allmond, and C. M. Himel. Affinity chromatography of acetylcholinesterase from *Electrophorus electricus* electroplax: investigation on 9-aminoalkylacridine affinity ligands. *J. Chromatogr.* **257**:275–284 (1983).
24. Ellman, G. L., K. D. Courtney, V. Andres, and R. M. Featherstone. A new rapid colorimetric determination of acetylcholinesterase activity. *Biochem. Pharmacol.* **7**:88–96 (1961).
25. Nabb, D. P., and F. Whitfield. Determination of cholinesterase by an automated pH-stat method. *Arch. Environ. Health* **15**:147–154 (1967).
26. Chan, L. M., C. M. Himel, and A. R. Main. Active-site-directed fluorescent probes in the kinetics and spectroscopy of purified horse serum cholinesterase. *Biochemistry* **13**:86–90 (1974).
27. Seitz, A., and C. M. Himel. Fluorescence analysis for esteratic, anionic and allosteric subsites of acetylcholinesterase. *Anal. Lett.* **10**:11–19 (1977).
28. Canellakis, E. S., Y. H. Shaw, W. E. Honners, and R. A. Schwartz. Diacridines: bifunctional intercalators. I. Chemistry, physical chemistry and growth inhibitory properties. *Biochim. Biophys. Acta* **418**:227–289 (1976).
29. Mooser, G., H. Schulman, and D. Sigman. Fluorescent probes of acetylcholinesterase. *Biochemistry* **11(9)**:1595 (1972).
30. Stryer, L. Fluorescence spectroscopy of proteins. *Science* **162**:526 (1968).
31. Hasan, F. B., S. G. Cohen, and J. B. Cohen. Hydrolysis by acetylcholinesterase. *J. Biol. Chem.* **255**:3898–3904 (1980).
32. Berman, H. A., and M. M. Decker. Kinetic, equilibrium and spectroscopic studies on cation association at the active center of acetylcholinesterase-topographic distinction. *Biochim. Biophys. Acta* **872**:125–133 (1986).
33. Albert, A. *The Acridines*. Edward Arnold, London, 170–171 (1966).
34. Taylor, P., J. L. Lwebuga-Mukasa, S. Lappi, and J. Rademacher. Propidium—a fluorescence probe for a peripheral anionic site on acetylcholinesterase. *Mol. Pharmacol.* **10**:703–708 (1974).
35. Berman, H. A., M. W. Decker, M. W. Nowak, K. J. Leonard, M. McCauley, W. M. Baker, and P. Taylor. Site selectivity of fluorescent bisquaternary phenanthridinium ligands for acetylcholinesterase. *Mol. Pharmacol.* **31**:610–616 (1987).
36. Radic, Z., E. Reiner, and P. Taylor. Role of the peripheral anionic site on acetylcholinesterase: inhibition by substrates and coumarin derivatives. *Mol. Pharmacol.* **39**:98–104 (1990).
37. Massoulie, J., L. Pezzementi, S. Bon, E. Kreijci, and F. M. Vallette. Molecular and cellular biology of cholinesterases. *Prog. Neurobiol.* **41**:55 (1993).
38. Rosenberry, T. L. Catalysis by acetylcholinesterase. The rate limiting steps involved in the acylation of acetylcholinesterase by acetic acid esters and phosphorylating agents. *Croatia Chem. Acta* **47**:235 (1975).

Send reprint requests to: Dr. Richard T. Mayer, USDA, ARS, SAA, Horticultural Research Laboratory, 2120 Camden Road, Orlando, FL 32803.